28.1 A Capacitive Touch Chipset with 33.9dB Charge-Overflow Reduction Using Amplitude-Modulated Multi-Frequency Excitation and Wireless Power and Data Transfer to an Active Stylus

Jae-Sung An[1], Jong-Hyun Ra[2], Eunchul Kang[1], Michiel A. P. Pertijs[1], Sang-Hyun Han[3]

[1]Delft University of Technology, Delft, The Netherlands
[2]SK hynix, Icheon, Korea
[3]Leading UI, Anyang, Korea

As the demand for high frame rate and SNR increases in capacitive touch systems (CTSs), several driving methods have been reported [1-5]. However, when excitation circuits simultaneously send excitation signals (V_{EXT}s) to multiple TX electrodes in order to increase frame rate, the readout circuit suffers from charge overflow because of the superposition of V_{EXT}s. To prevent this, driving methods such as time-division [1,5] and reduced-amplitude excitation [3], and signal omitting and linear interpolation in the digital domain [4] have been adopted in AFE ICs, but they degrade the frame rate, and SNR, and increase the computational load of the CTS, respectively. In this paper, amplitude-modulated multiple-frequency excitation (AM-MFE) is used to prevent charge overflow without degrading the frame rate, SNR, and computational load. In addition, an electric pencil case (EPC) is proposed for wireless power and data transfer to an active stylus, so as to avoid the need to replace the battery of the stylus or charge it via an adapter.

Figure 28.1.1 shows a block diagram of the CTS with EPC. The CTS consists of the touch screen panel (TSP), an AFE IC that includes the excitation and readout circuits and an FFT processor, and a MCU to control the AFE IC (MCU_AFE). In addition, the EPC consists of an interface (I/F_EPC), MCU (MCU_EPC), a wireless power and data transceiver (WPDT), a battery, and an EPC coil. When the active stylus is in the EPC, the power level that needs to be delivered to the stylus is determined by the MCU_EPC based on stylus data (D_{STY}) transferred to the WPDT via the stylus and EPC coils. To minimize the impact of external interfering signals, which feed into the AFE IC via the TSP, on the detected stylus coordinates and other functionalities, the MCU_AFE observes the interference spectrum and locates the excitation frequencies ($f_{EXT1\text{-}N}$) and the stylus frequency (f_S) in the low-noise region. The stylus frequency is wirelessly transferred to the MCU_EPC.

To prevent charge overflow, which occurs periodically at the beat frequency of the f_{EXT}s, the MCU_AFE decides a mix frequency (f_{MIX}) by considering the distribution of f_{EXT}s, and sends this to the AFE IC to reduce the amplitudes of V_{EXT}s with the same periodicity. To do so, the excitation circuits generate the amplitude-modulated V_{EXT}s at f_{MIX}, and provide the resulting signals to the TX electrodes of the TSP. The readout circuit receives the resulting charge signal (Q_S) from the TSP without charge overflow. Thus, the readout circuit senses the Q_S maintaining the frame rate, while maximizing the amplitude of Q_S up to the sensing range to improve SNR.

Figure 28.1.2 shows a block diagram of the AFE IC. The AFE IC consists of an N-channel excitation circuit, an M-channel readout circuit, an FFT processor, and an LVDS link. Each channel of the excitation circuit includes a direct digital synthesizer (DDS), an LPF, a mixer, controlled by a shared mixer controller, and a PGA. Each readout channel contains a second-generation current conveyor (CCII) and a HPF. Groups of 4 channels share an ADC by means of a 4:1 MUX. In the excitation circuit, the DDS and LPF generate a sinusoidal signal. The mixer modulates this signal at f_{MIX}. The PGAs amplify the resulting signals so as to maximize the sensing range and drive the TX electrodes. The readout circuit adopts a differential sensing method and filtering to attenuate external interfering signals, which are dominantly distributed up to tens of kHz [3,5]. The differential sensing is realized by connecting the CCII outputs ZP and ZN between two adjacent channels. In addition, the combination of TSP and CCII, which operates as a 1st-order BPF, and a 2nd-order HPF are designed to have a cut-off frequency of 100kHz [3]. The output resistors of the CCIIs control the signal gain. Since the fabricated 32" TSP has a 1.5MHz cut-off frequency and 4:1 MUXes are used, the 12b ADCs are designed to operate at a sampling rate of 12MHz to meet the Nyquist theorem. In every readout circuit, the 1024 12b ADC data are transferred from the 12b ADC to the memory in the FFT processor, and then the 1024-point FFT processor converts them to 1024 FFT data (D_{FFT}) in parallel, which is distributed within ±1.5MHz. Thus, the AFE IC achieves a frame rate of 2.93kHz. In the FFT data, when f_{MIX} is chosen equal to $f_d/2$, only the frequencies of f_1-f_{MIX} and f_N+f_{MIX} are detected because other frequencies are superposed to be approximately zero. The AFE_MCU recovers the information at $f_{EXT1\text{-}N}$ by summing two adjacent frequencies without heavy computational load.

Figure 28.1.3 (top) shows the schematic and timing diagrams of the excitation circuit. AM is performed using an operational amplifier with a programmable feedback network consisting of C_{MIX1}, C_{MIX2} and chopper switches. To set the magnitude of the gain, the value of C_{MIX1} is controlled by D<7:0>, while the polarity is set by switching between an inverting and non-inverting feedback configuration using chopper switches controlled by D_{CHOP}. The PGA amplifies V_{MIX} and provides the resulting V_{EXT} to the TSP. Figure 28.1.3 (bottom) shows the measurement results of Q_S. Without the AM-MFE, charge overflow occurs because of superposition of V_{EXT}s having $f_{EXT1\text{-}N}$. Therefore, it is hard to enhance the SNR by increasing the amplitude of V_{EXT}s. Since the charge overflow occurs periodically at the beat frequency of f_{EXT}s, f_{MIX} determined by the MCU_AFE based on the distribution of f_{EXT}s to reduce the excitation amplitude with the same periodicity. When the f_{EXT}s are uniformly distributed, this AM-MFE scheme reduces the peak amplitude of Qs by 33.89dB. When prime-number frequency spacing is used, which helps to reduce charge overflow, AM-MFE still reduces the peak amplitude by 5.87dB. Considering the differences of amplitude of Q_Ss between with and without the AM-MFE, the amplitude of V_{EXT}, which is directly proportional to the SNR, can be increased up to 33.89dB and 5.87dB when the equal and prime-number frequency spacing are used, respectively. However, in the AFE IC, the PGA is designed using 5V devices in order to reduce the power consumption and to avoid the high-voltage device, which requires the large area and cost, and thus it can increase the amplitude of V_{EXT} from 3.3V (w/o AM-MFE) to 5V (w/ AM-MFE) resulting the SNR improvement without degrading the frame rate. After then, the CCII in the readout circuit adjusts the amplitude of the output signal according to the signal range of ADC for achieving the large dynamic range.

Figure 28.1.4 shows a block diagram of the EPC and active stylus. In the EPC, the WPDT integrates memory, a TX controller, a charge pump, an interface to the MCU_EPC, and 3-TRX core blocks including a comparator, a rectifier and an LPF, a current detector, an FSK modulator, and a gate driver. FSK is used to send data to the stylus, and ASK is used to receive data (D_{STY}) from the stylus [6]. When the active stylus sends D_{STY} using an ASK method to WPDT, the current detector senses the current (I_{TX}), which is then rectified, low-pass filtered and compared with a threshold to reconstruct D_{STY}, which is sent to the MCU_EPC. Based on this, the MCU_EPC controls the gate driver and full-bridge inverter to wirelessly transfer power to the active stylus at 80.2% maximum efficiency. To set the f_S at which stylus operates, D_{EPC} is wirelessly transferred to the active stylus using FSK. Due to the resonance frequency of stylus coil, the amplitude of transferred signal is varied according the frequency, and thus the active stylus can detect the D_{EPC}. To use multiple active stylus, the 3-TRX cores allow wireless power and data transfer to multiple styli by differentiating the ID of the stylus.

Figure 28.1.5 (left) shows the measurement setup for the CTS. The CTS is implemented with a 32" TSP. Because a differential sensing method is used in the AFE IC, the most display noise is filtered out [2-5]. The AFE IC with AM-MFE has slightly lower SNR than without AM-MFE at the same amplitude of V_{EXT} due to the amplitude variation of V_{EXT}, but it has no amplitude of V_{EXT} limitation due to the charge overflow related to the SNR. In addition, the Q_S is amplified by the CCII to maximize the dynamic range for the sensing period. Figure 28.1.5 (right) shows the frequency spectra of AM-MFE with equal frequency spacing of f_{EXT}s. When the MCU_AFE receives the D_{FFT}, it demodulates the D_{FFT} by sequentially summing two adjacent FFT data from f_1-f_{MIX} to f_{64}+f_{MIX} Thus, MCU_AFE extracts the coordinates of finger and styli without the charge overflow and low computational load.

Figure 28.1.6 compares the performance of the AFE IC with the state of the art. The AFE IC using the AM-MFE reduces the charge overflow up to 33.9dB, which is the highest value among the previous works. The EPC transfers the power with 80.2% efficiency and data to the active stylus. The AFE IC and the WPDT were realized in a 0.13μm CMOS process. Figure 28.1.7 shows the photomicrographs and the specifications for the WPDT.

Acknowledgements:
We thank Prof. Kwon of Hanang University for the helpful discussions. The authors also thank MNtech Co., Ltd. for supporting capacitive touch sensors.

References:
[1] C. Park et al., "A Pen-Pressure-Sensitive Capacitive Touch System Using Electrically Coupled Resonance Pen," *ISSCC*, pp. 124-125, Feb. 2015.
[2] M. Hamaguchi et al., "A 240Hz-Reporting-Rate Mutual-Capacitance Touch-Sensing Analog Front-End Enabling Multiple Active/Passive Styluses with 41dB/32dB SNR for 0.5mm Diameter," *ISSCC*, pp. 120–121, Feb. 2015.
[3] J.-S. An et al., "A 3.9kHz-Frame-Rate Capacitive Touch System with Pressure/Tilt Angle Expressions of Active Stylus Using Multiple-Frequency Driving Method for 65" 104×64 Touch Screen Panel," *ISSCC*, pp. 168-169, Feb. 2017.

 978-1-7281-3205-1/20/$31.00

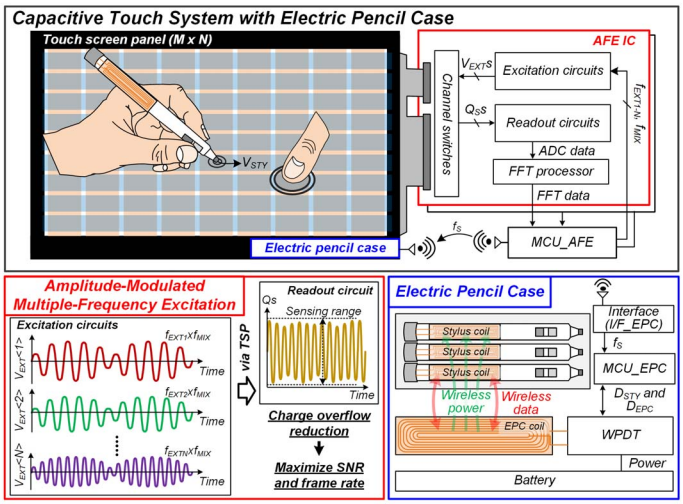

Figure 28.1.1: Block diagram of the proposed capacitive touch system (CTS) with electric pencil case (EPC).

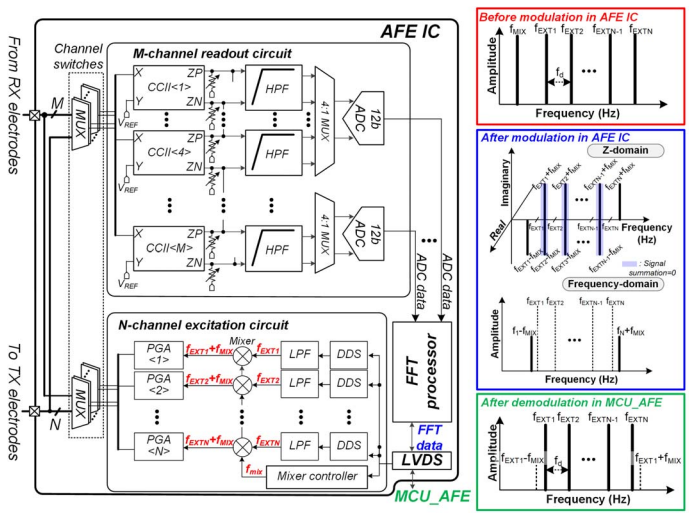

Figure 28.1.2: Block diagram of the AFE IC.

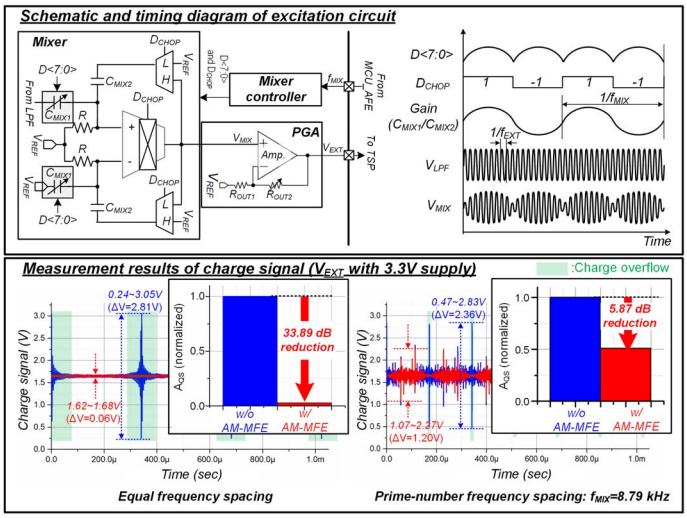

Figure 28.1.3: Schematic and timing diagram of the excitation circuit (top) and measured results for the charge signal (bottom).

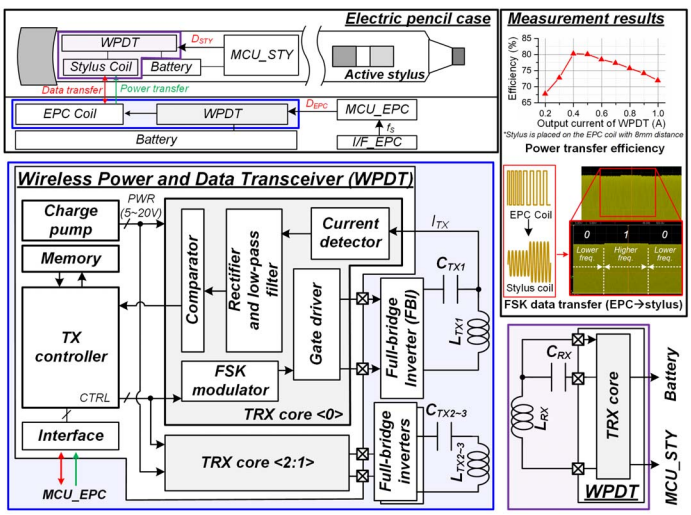

Figure 28.1.4: Block diagram of the electric pencil case (EPC) and stylus.

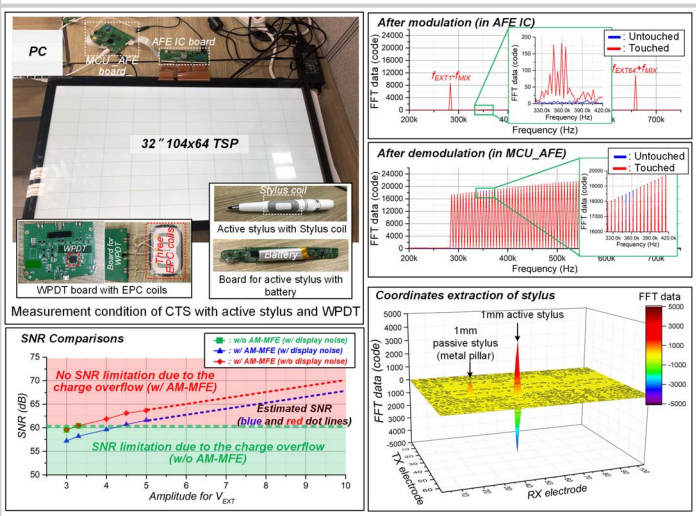

Figure 28.1.5: Measurement setup for the CTS with an active stylus and WPDT (left-top), SNR comparison (left-bottom), frequency spectra of AM-MFE (right-top), and coordinate extraction for the stylus (right-bottom).

		This work	ISSCC 2014 H. Jang et al.	ISSCC 2015 [1]	ISSCC 2017 [3]	ISSCC 2018 [4]	ISSCC 2018 [5]	JSSC 2019 J.-E. Park et al.
Process		0.13-μm CMOS	0.18-μm CMOS	0.18-μm BCD	0.13-μm CMOS	100-nm CMOS	0.13-μm CMOS	0.18-μm CMOS
TSP size		32-inch[1]	4.8-inch	10.1-inch	65-inch	10.1-inch	86-inch	12.2-inch
# of electrodes		104 × 64	24 × 16	48 × 32	104 × 64	54 × 35	198 × 112	64 × 36
Electrode		Metal Mesh	N/A	ITO	Metal Mesh	Metal mesh	Metal mesh	ITO
Frame rate		2.93 kHz	160 Hz	240 Hz	3.9 kHz	133 Hz	977 Hz	85~385 Hz
Charge overflow reduction method		Amplitude-Modulated Multi-Frequency Excitation	Q_S cancellation method at the charge overflow period	Time division	Reduced-amplitude excitation	Signal omitting and linear interpolation method (digital)	Time division	Modified orthogonal matrices
Maximum charge overflow reduction ratio		33.89 dB	N/A	N/A	N/A	N/A	6.02 dB	13.98 dB
SNR	Metal pillar (Φ=1mm)	41.7 dB	N/A	49.0 dB	41.0 dB	56.0 dB	39.0 dB	41.0 dB (@120 Hz frame rate)
	Finger[2] (Φ=10 mm)	61.6 dB	53 dB	62.0 dB (Φ=6 mm)	61.0 dB	N/A	60.1 dB	54.0 dB (@120 Hz frame rate)
Stylus	Type	Active	-	Electrically Coupled Resonance (ECR)	Active	Electrically Coupled Resonance (ECR)	Active	-
	Wireless power and data transfer	Yes (Electric pencil case)	-	-	No	-	No	-
Supply		1.5 / 3.3 / 5.0 V	1.8 / 3.3V	N/A	1.5 / 3.3 V	N/A	1.5 / 3.3 V	2.7~3.3V
Power consumption		290.8 mW	2.6 mW (Analog)	30.0 mW	246.3 mW	24.0 mW	797.4 mW	94.5 mW (@3.3V) 67.7 mW (@1.8/3.3V)
Chip area		72.25 mm²	0.46 mm²	14.7 mm²	42.25 mm²	39.2 mm²	74.17 mm²	36.0mm²

[1]32" 104 × 64 TSP using a mesh structure, of which both the TX and RX electrodes have a 10.0μm thickness Ag with a sheet resistance of less than 4.0Ω/□. The TSP is covered with a 3.0mm thickness cover glass and mounted on the LCD display with a 2.0mm air gap.
[2]SNR of AFE IC is measured with 5.0V V_{EXT}s and display ON.

Figure 28.1.6: Performance comparison of the AFE IC with the state of the art.

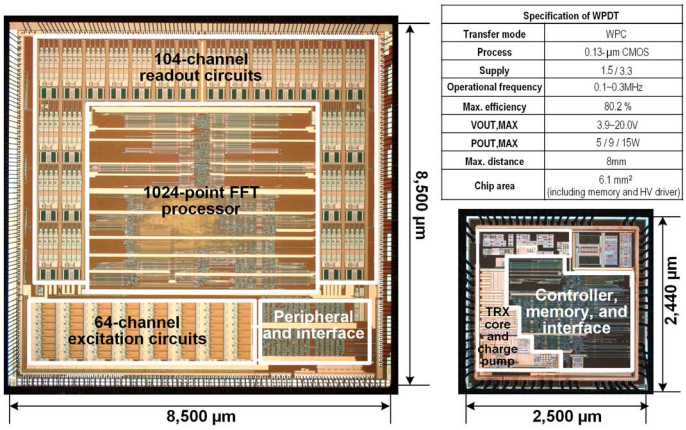

Specification of WPDT	
Transfer mode	WPC
Process	0.13-µm CMOS
Supply	1.5 / 3.3
Operational frequency	0.1~0.3MHz
Max. efficiency	80.2 %
VOUT,MAX	3.9~20.0V
POUT,MAX	5 / 9 / 15W
Max. distance	8mm
Chip area	6.1 mm² (including memory and HV driver)

Figure 28.1.7: Photomicrograph of the AFE IC (left) and wireless power and data transceiver with its specifications (right).

- ***Quantitative Analysis of Charge Overflow: without AM-MFE***

- $Qs = \Sigma_{i=0}^{n-1} \sin(f_l + i \cdot f_d)$,
  - f_l: lowest freq.
  - f_d: frequency step
  - n: number of V_{EXT}s

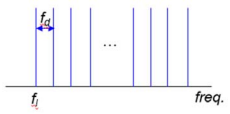

$$Qs = \Sigma_{i=0}^{n-1} \sin(f_l + i \cdot f_d)$$
$$= \sin(f_l) + \sin(f_l + f_d) \qquad \Rightarrow 2 \cdot \sin(f_l + 1/2 \cdot f_d) \cdot \cos(f_d/2)$$
$$+ \sin(f_l + 2f_d) + \sin(f_l + 3f_d) \qquad \Rightarrow 2 \cdot \sin(f_l + 5/2 \cdot f_d) \cdot \cos(f_d/2)$$
$$+ \sin(f_l + 4f_d) + \sin(f_l + 5f_d) \qquad \Rightarrow 2 \cdot \sin(f_l + 9/2 \cdot f_d) \cdot \cos(f_d/2)$$
$$+ \ldots$$
$$+ \sin(f_l + (n-2)f_d) + \sin(f_l + (n-1)f_d) \Rightarrow 2 \cdot \sin(f_l + (2n-3)/2 \cdot f_d) \cdot \cos(f_d/2)$$
$$= 2 \cdot \cos\left(\frac{f_d}{2}\right) \Sigma_{i=0}^{n/2-1} \sin\left(f_l + \frac{(4i+1)}{2} f_d\right)$$
$$= 4 \cdot \cos\left(\frac{f_d}{2}\right) \cdot \cos(f_d) \cdot \Sigma_{i=0}^{n/4-1} \sin\left(f_l + \frac{(8i+3)}{2} f_d\right)$$
$$= 8 \cdot \cos\left(\frac{f_d}{2}\right) \cdot \cos(f_d) \cdot \cos(2f_d) \cdot \Sigma_{i=0}^{n/8-1} \sin\left(f_l + \frac{(16i+7)}{2} f_d\right)$$

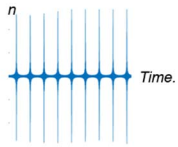

If $n = 2^k$

$$Qs = \Sigma_{i=0}^{n-1} \sin(f_l + i \cdot f_d)$$
$$= 2^k \cdot \sin\left(f + \frac{\Sigma_{i=0}^{k-1} 2^i}{2} f_d\right) \cdot \Pi_{i=0}^{k-1} \cos(2^{i-1} \cdot f_d)$$
$$= 2^k \cdot \sin\left(f + \frac{2^k - 1}{2} f_d\right) \cdot \Pi_{i=0}^{k-1} \cos(2^{i-1} \cdot f_d)$$

Amplitude of charge signal depends of the number of V_{EXT}s

Figure 28.1.S1: Quantitative analysis of charge overflow (without AM-MFE and equal frequency spacing).

- ***Quantitative Analysis of Charge Overflow: with AM-MFE***

- $Qs, proposed = \sin\left(\frac{1}{2} f_d\right) \cdot Qs$

$$= \sin\left(\frac{1}{2} f_d\right) \cdot 2^k \cdot \sin\left(f_l + \frac{2^k - 1}{2} f_d\right) \cdot \Pi_{i=0}^{k-1} \cos(2^{i-1} \cdot f_d)$$
$$= 2^k \cdot \sin\left(f_l + \frac{2^k - 1}{2} f_d\right) \cdot \sin\left(\frac{1}{2} f_d\right) \cdot \cos\left(\frac{1}{2} f_d\right) \cdot \Pi_{i=1}^{k-1} \cos(2^{i-1} \cdot f_d)$$
$$= 2^k \cdot \sin\left(f_l + \frac{2^k - 1}{2} f_d\right) \cdot \frac{1}{2} (\sin(f_d) + \sin(0)) \cdot \Pi_{i=1}^{k-1} \cos(2^{i-1} \cdot f_d)$$
$$= 2^k \cdot \sin\left(f_l + \frac{2^k - 1}{2} f_d\right) \cdot \frac{1}{2} \sin(f_d) \cdot \cos(f_d) \cdot \Pi_{i=2}^{k-1} \cos(2^{i-1} \cdot f_d)$$
$$= 2^k \cdot \sin\left(f_l + \frac{2^k - 1}{2} f_d\right) \cdot \frac{1}{2^2} \sin(2f_d) \cdot \Pi_{i=2}^{k-1} \cos(2^{i-1} \cdot f_d)$$
$$\ldots$$
$$= 2^k \cdot \sin\left(f_l + \frac{2^k - 1}{2} f_d\right) \cdot \frac{1}{2^k} \sin(2^{k-1} f_d)$$
$$= \sin\left(f_l + \frac{2^k - 1}{2} f_d\right) \cdot \sin(2^{k-1} f_d)$$
$$= \frac{1}{2} \left(\cos\left(f_l - \frac{1}{2} f_d\right) - \cos\left(f_l + \left(2^k - \frac{1}{2}\right) f_d\right) \right)$$

Amplitude of charge signal maintains up to 1

Figure 28.1.S2: Quantitative analysis of charge overflow (with AM-MFE and equal frequency spacing).

- ***Conceptual Diagram for the Proposed AM-MFE***

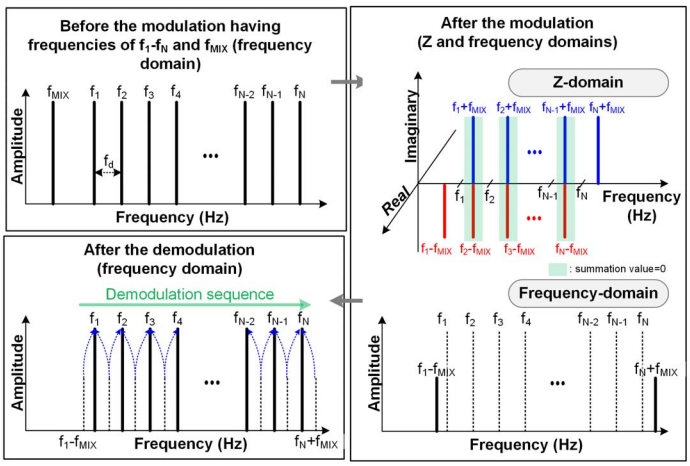

Figure 28.1.S3: Conceptual diagram for the AM-MFE in frequency/Z-domains.

Additional References:
[4] K.-H. Lee et al., "A Noise-Immune Stylus Analog Front-End Using Adjustable Frequency Modulation and Linear-Interpolating Data Reconstruction for Both Electrically Coupled Resonance and Active Styluses," *ISSCC*, pp. 184-185, Feb. 2018.
[5] J.-S. An et al., "Multi-way Interactive Capacitive Touch System with Palm Rejection of Active Stylus for 86" Touch Screen Panels," *ISSCC*, pp. 168-169, Feb. 2017.
[6] Wireless Power Consortium. Qi Specifications [Online]. Accessed on Aug. 20, 2019. Available: https://www.wirelesspowerconsortium.com/knowledge-base/specifications/download-the-qi-specifications.html

978-1-7281-3205-1/20/$31.00 ©2020 IEEE